CONSTRUCTION OF FAULT EVOLUTION MAPS FOR DAMAGE LEVEL ASSESSMENT OF RAILWAY BEARINGS

CÉSAR RICARDO SOTO-OCAMPO[1], JUAN DAVID CANO-MORENO[2] & JOSÉ MANUEL MERA[1]
[1]Railway Technology Research Center (Centro de Investigación en Tecnología Ferroviaria-CITEF), Universidad Politécnica de Madrid, Spain
[2]Escuela Técnica Superior de Ingeniería y Diseño Industrial, Universidad Politécnica de Madrid, Spain

ABSTRACT
The diagnosis of the state of machinery is becoming increasingly important in a more competitive industrial sector. Therefore, maintenance strategies are essential to ensure the correct and continuous operation of equipment. In the last decade, the application of condition based monitoring (CBM) has increased significantly in the detection of bearing faults. CBM is based on the characterisation of equipment behaviour and focuses on preventing a machine from failing. Therefore, fault characterisation and the construction of health indicators is a fundamental issue in CBM. This study evaluates the performance of the diagnostic methodology based on the construction of contour maps from envelope spectra. This allows the construction of visual maps that characterise the evolution of the amplitude of a fault frequency and its harmonics. They also serve as a reference to establish health indicators of future equipment conditions. The results suggest that the methodology holds promise for bearing condition classification. Furthermore, the use of contour maps is a visually intuitive tool for the analyst.
Keywords: contour map, condition monitoring, bearing diagnosis, envelope analysis.

1 INTRODUCTION

Increasing industrial progress has driven the development and evolution of maintenance strategies. These are focused on ensuring the correct and continuous operation of machinery, especially of the most critical components, such as bearings [1], [2]. One of the maintenance strategies with the greatest projection in the diagnosis and prognosis of the condition of mechanical equipment is condition based monitoring (CBM) [3]–[5], due to the availability of data processing techniques.

Using mainly vibration signals [6], CBM studies the state of the machine during its entire operating interval, to extend the life of the different components, reduce downtime and optimise the maintenance schedule. In other words, CBM focuses on identifying the cause of the failure to prevent it from occurring. Therefore, the characterisation of behavioural patterns and the construction of health indicators plays an important role in machine condition assessment tasks. This has created many studies focused on the extraction of features that allow the construction of classifiers of the state of a machine, mainly based on artificial intelligence or signal processing [7].

In recent years, studies developed using artificial intelligence have increased significantly, where surface learning and deep learning algorithms are protagonists in the detection, diagnosis, and prognosis of bearings [2], [3], [8]–[11]. On the other hand, an increase in studies associated with traditional vibration signal processing techniques is also evident in the literature [7], [12]–[14]. In these studies, envelope analysis takes centre stage in the demodulation of resonant zones of signals associated with frequencies of bearing failures. Moreover, a novel methodology based on contour maps has been presented for the characterisation and construction of fault evolution maps, which serve as a reference in the diagnosis of bearings [14].

WIT Transactions on The Built Environment, Vol 213, © 2022 WIT Press
www.witpress.com, ISSN 1743-3509 (on-line)
doi:10.2495/CR220051

The main objective of this work focuses on the evaluation of the performance of the bearing diagnosis methodology based on contour maps, presented in Soto-Ocampo et al. [14]. Contour maps are graphical illustrations used to represent spatial functions by incorporating isolines. This criterion has allowed characterising the behavioural pattern of a bearing defect, considering the changes experienced by the amplitude of the fault frequency and harmonics over time. Therefore, the construction of these fault evolution maps makes it possible to establish a relationship with any machine condition.

2 METHODOLOGY

2.1 Basis of the methodology

The approach of using contour maps as a method of vibration mode characterisation arises from considering the oscillatory fundamentals of rolling bearings.

2.1.1 Vibration mode of rolling bearings

Bearings are mechanisms that have their own mode of vibration, generated by the contact of the components that make them up and interpreted through their frequencies. From this, a relationship is established between the geometry of the components and the energy developed in the passage of the rolling elements through the load zone [15]. Consequently, irregularities in the surface generate changes in the contact stresses of the components of a bearing, resulting in the generation of very short duration pulses that excite the natural frequencies of the entire structure [6], [16], [17]. Thus, the vibration signature of a bearing establishes the relationship between the magnitude of the irregularity and the amplitude of the generated pulse, manifested in the characteristic frequency of the failure component (Fig. 1).

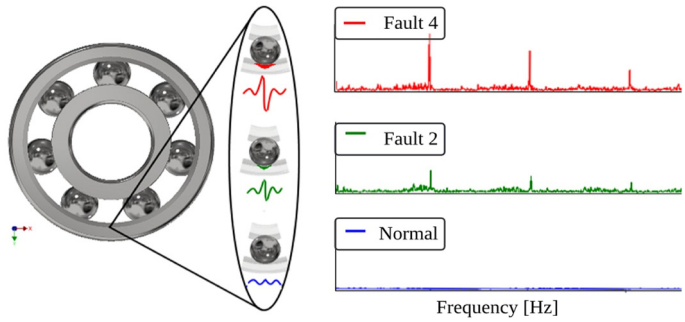

Figure 1: Envelope spectra representation of fault evolution.

2.1.2 Contour maps

As mentioned above, signal spectra can identify frequencies associated with a fault component and its respective amplitude. However, the main drawback arises at the time of diagnosis. There is a lack of criteria to evaluate the state of the components of a bearing and to relate them to a fault level. However, the use of contour maps [14] allows to characterise the behavioural pattern of a bearing defect, by relating the failure frequency of a component to the amplitude changes it experiences as the failure level increases.

Contour maps are graphical illustrations used to represent spatial functions by incorporating isolines [18]. Each isoline has a constant and equally spaced contour value

(associated with an amplitude value) [19], [20]. In this way, the isolines allow to classify and separate the points of the underlying space, generated by amplitude changes of a fault, establishing a direct relationship between the fault frequency, its amplitude and the corresponding fault level. Fig. 2 represents the contour map characterising the amplitude changes of a fault frequency over time.

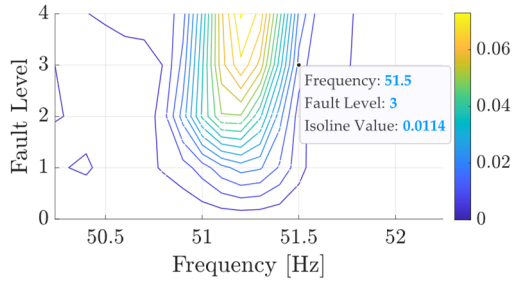

Figure 2: Representation of the coordinates of the points that form the isolines.

In the spectral analysis of a record to be evaluated, information is obtained from two of these components (fault frequency and amplitude) named analysis points from now on. The objective of the methodology is to determine the relationship of the analysis points of a spectrum with the fault level to which it corresponds within the fault evolution map. Therefore, the spectrum to be compared in the contour map must be evaluated according to the values of the isolines of the fault evolution map, thus obtaining the analysis points.

2.2 Basis of the methodology

The development of the proposed methodology is structured in six phases, which have been detailed in Soto-Ocampo et al. [14]. However, this article presents changes in obtaining the threshold value and considers measures of central tendency to estimate the relationship of a spectrum with its failure level. The methodology is presented below in the flow chart in Fig. 3.

2.2.1 Data acquisition

The data acquisition phase comprises the instrumentation of the equipment under study and the capture of vibration records. This phase is carried out in two scenarios. Initially, it is necessary to have records describing the evolution of the failure of a bearing component over time. These should allow the construction of the failure evolution maps. In this scenario it is important to determine up to what level the deterioration of a failure is considered permissible for continued operation. On the other hand, the second scenario refers to the records that are analysed or related to the fault evolution maps.

2.2.2 Determination of representative samples

It is important to ensure that the samples of the records that make up the fault evolution map and the record to be diagnosed, have:

1. Constant rotational speed,
2. Homogenisation of fault frequency, and
3. Same frequency resolution.

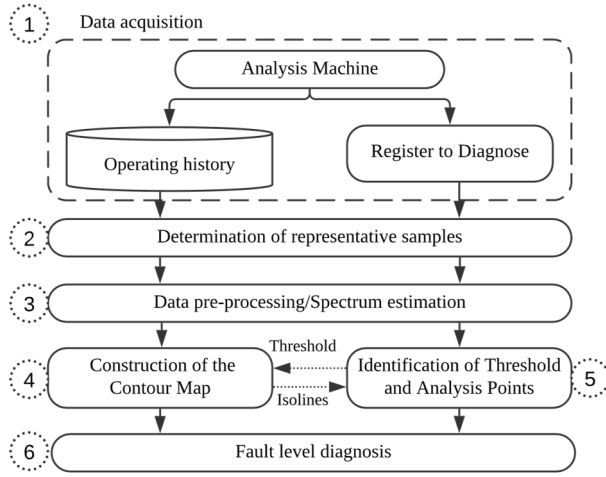

Figure 3: Structure of the methodology.

Fernández-Francos et al. [21] stresses the importance of maintaining a constant rotational speed in record capture. This is to eliminate frequency lags and variations in impact force. Regarding the homogenisation of the failure frequency, this criterion reduces the uncertainty in the identification of the failure frequency. Smith and Randall [22] consider a variation of the frequency calculation between 1% or 2%. It is also important to maintain the same frequency resolution, so the samples that make up the fault evolution map and the one to be evaluated must have the same length in time [23].

2.2.3 Data preprocessing

Gupta and Pradhan [17], suggest that the data processing technique used in the analysis should be selected according to the component under study. Therefore, considering the oscillatory fundamentals of the bearing, this study uses the "Envelope Analysis" technique, as it mainly seeks to detect resonant zones excited or modulated in amplitude by periodic impact forces, whose repetition frequency is an indicator of the location of the defect and its amplitude a measure that characterises the state of the component [24]. The application of this analysis technique includes:

1. Frequency band selection,
2. Signal filtering,
3. Extraction of the envelope signal (using Hilbert Transform), and
4. Construction of the Envelope Spectrum.

Some studies describe the importance of identifying the frequency band with the most information about the condition of a bearing [16], [25]. However, in this study, a constant filtering band of 1.8–6.1 kHz is considered [26]; this is to avoid signal attenuation due to changes in the selection of the filtering band.

2.2.4 Construction of the fault evolution map

In the construction of fault evolution maps there are three key parameters to consider, as follows:

1. Lower limit or threshold
2. Upper limit,
3. Contour interval.

The estimation of the *Threshold* corresponds to the lowest isoline value and allows the identification of the most representative amplitudes of the signal. Since the main objective of the methodology is to evaluate records of different fault levels, it is considered that this value should be adapted to the behaviour of the record under study. Therefore, the Threshold value is provided by the record to be diagnosed. In Soto-Ocampo et al. [14], the estimation of this parameter was performed by implementing a series of processes, however this process entails a higher computational expense. In this work, the estimation of the Threshold value is performed in three steps:

1. Determination of the mean ($\bar{x}$) of the sample (x), corresponding to the data of the spectrum with length N,

$$\bar{x} = \frac{\sum_{i=1}^{N} x_i}{N} \tag{1}$$

2. Identification of the peaks (P_e) of the sample, whose amplitude exceeds the mean of the signal ($\bar{x}$),

$$P_e = Peak(x) \geq \bar{x} \tag{2}$$

3. Threshold estimate, equivalent to the median (M_e) of the amplitude of the peaks identified in (6), where N_{P_e} represents the number of peaks identified.

$$M_e = \begin{cases} P_{e\frac{N_{P_e}+1}{2}} & N_{P_e}\ odd \\ \dfrac{P_{e\frac{N_{P_e}}{2}} + P_{e\frac{N_{P_e}+1}{2}}}{2} & N_{P_e}\ even \end{cases} \tag{3}$$

The *Upper Boundary* ($Upper_{Boundary}$) is associated with the maximum amplitude of the fault frequency, or harmonics, of the spectra that make up the fault evolution map. This limit represents the maximum value for isolines fault evolution map.

The Contour Interval (C_i) represents the spacing value between isolines. It is therefore important to define the number of isolines (N_{iso}) used in the construction of the contour maps, which in turn allows to define the values of each isoline ($Isoline_{Value}$). This process is carried out in three stages:

1. In the determination of the N_{iso} the Sturges rule [27] is considered, this rule is simple and is adjusted to the number of samples (N) of the spectrum analysed,

$$N_{iso} = 1 + 3.322 \cdot log_{10}(N) \tag{4}$$

2. Calculation of the contour interval,

$$C_i = \frac{Upper_{Boundary} - Threshold}{N_{iso}} \tag{5}$$

3. The value of each isoline ($Isoline_{Value}$) is defined by a set of values, set by the multiples of the contour and threshold interval, without exceeding the upper limit. This relationship is presented below, where k = 0,1,2,3,..., represents the multiple of the spacing value.

$$Isoline_{Value} = Threshold + k \cdot C_i \tag{6}$$

2.2.5 Treatment of the record to be evaluated

As in the construction of the fault evolution maps, the record to be diagnosed is evaluated according to the estimated isoline values. This makes it possible to identify the analysis points associated with the intersection of the isoline values and the amplitude of the frequency under study, as shown in Fig. 4.

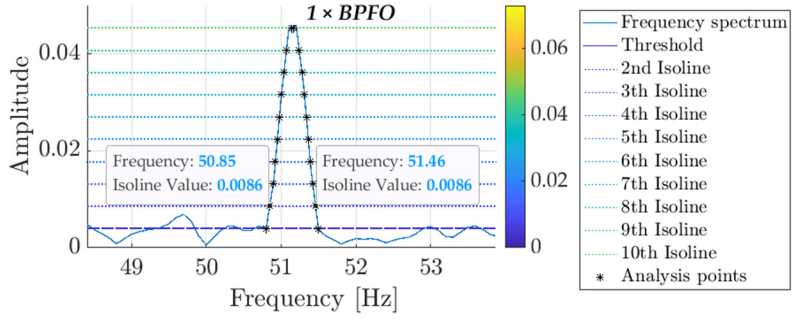

Figure 4: Identification of the analysis points (recording at 500 rpm and fault level F2).

In this way, the analysis points identify two coordinates, frequency and amplitude, associated with each isoline value. Fig. 5 presents the coordinates of two of the analysis points P1 (50.85, 0.0086) and P2 (51.46, 0.0086), associated with the intersection of the fault frequency amplitude with the second isoline.

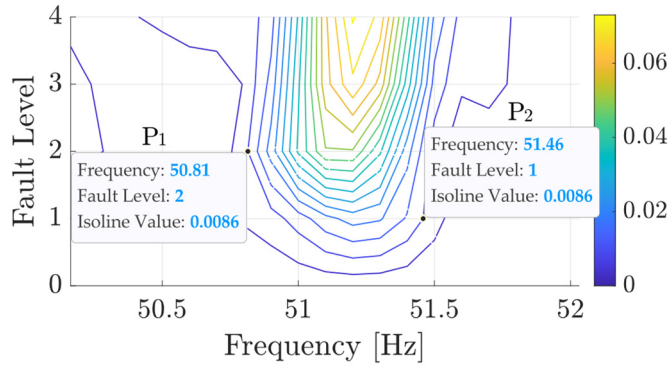

Figure 5: Relationship between the analysis points (P1 and P2) and their isoline.

2.2.6 Fault level diagnosis

It is known beforehand that each of the isolines of the fault evolution map is associated with an amplitude level, and that the points that form it have coordinates in frequency and fault level. Therefore, by defining the isoline of the fault evolution map to which each point of analysis corresponds and identifying its frequency, the relationship with the corresponding fault level is visualised.

Fig. 5 presents the relationship between the analysis points P1 and P2 (see Fig. 4), and the corresponding isoline points of the fault evolution map. This analysis was carried out by frequency approximation. Once the isoline was selected, the frequency coordinate of the analysis points was identified in the coordinates of the isoline points, looking for the corresponding frequency or the closest frequency. From this analysis, a relationship of P1 and P2 was established with a fault level of 2 and 1 respectively.

The isolated analysis of points P1 and P2 could be considered confusing, given their relationship with different fault levels. However, when considering the totality of the analysis points for each harmonic of the fault frequency, the trend over a fault level F2 is clearly observed, as presented in Fig. 6.

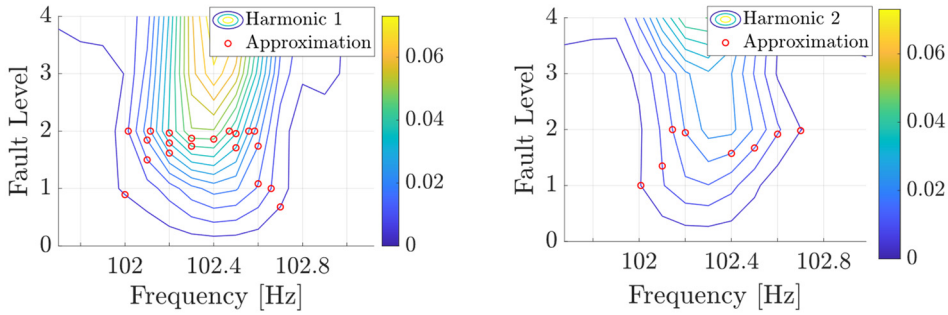

Figure 6: Relationship between the analysis points and the fault evolution map.

As observed in Fig. 6, the diagnosis of a spectrum on a fault evolution map is visually intuitive, as the fault level trend of each harmonic is marked by a point cloud. In the quantification of the fault level trend, central tendency measures, such as mean and median, are considered. Thus, from the data set defined by the point cloud of each harmonic the trend or fault level is established. The evaluation of the trend of the fault level of the spectrum at 500 rpm and labelled with fault level F2 (see Fig. 4), is estimated at 1.93 and 1.87 by means of the mean and median respectively.

3 EXPERIMENTAL DATA

The data set used in this study to evaluate the performance of the proposed methodology was obtained from the bearing test rig of the Railway Technology Research Center (CITEF) [28]. Since the methodology has been devised for the diagnosis of railway axlebox bearings, the bearings in the test rig housings have a similar configuration. Also, the evaluation regimes have been considered according to the angular velocity profile of the wheels of a metro train.

The test bearing used is a double row spherical roller bearing. The records were evaluated at three different speeds (200, 350, 500 rpm). Their characteristic failure frequencies as ball pass frequency inner (BPFI), ball pass frequency outer (BPFO), ball spin frequency (BSF) and fundamental train frequency (FTF), are presented in Table 1.

Table 1: Estimating the level of failure by measures of central tendency.

22205E1KC3				Units
Regime	200	350	500	rpm
BPFO	20.62	36.08	51.54	Hz
BPFI	29.38	51.42	73.46	Hz
BSF	18.01	31.52	45.03	Hz
FTF	1.37	2.41	3.44	Hz

A combined rolling element (RE) and outer race (OR) failure was induced in the bearing, evaluated at five failure levels including the normal state (F0, F1, F2, F3, F4). The generated damage ranged in depth from 0.006 to 0.027 mm for RE, and 0.007 to 0.028 (mm) for OR. Each case study was repeated three times, where the most representative replica was used to construct the failure evolution map.

The data acquisition equipment used is based on low-cost components developed for condition monitoring of rotating machinery [26]. The acceleration signals were obtained at a sampling frequency of 45 kHz. Each record has a length of 45 seconds.

4 RESULTS

This section presents the results of the bearing diagnosis using the proposed methodology. Given the length of each record (45 seconds) and considering the criteria for selecting representative samples, each record was evaluated in a window with a length of 5 seconds, which allows several samples to be available for each record. In addition, with the proposed window length, a frequency resolution of 0.1 Hz is obtained, which guarantees to distinguish between close frequencies. It should be noted that the samples used in the construction of the fault evolution maps are not considered for the diagnosis and validation of the methodology.

Although the records are associated with a combined fault (ORRE), in this study the evaluation of the performance of the methodology focuses on the fault associated with the outer track.

4.1 Use of isolines for spectra evaluation

The arrangement of the isolines that make up the fault evolution map establishes a pattern of scales that allow the amplitudes of the spectrum under study to be analysed.

Fig. 7 presents the use of the isoline values as a scaling pattern on which to evaluate the record under study (record at 500 rpm and fault level F2). As can be seen, the maximum peak of the evaluated spectrum intersects with the tenth isoline. Therefore, from this analysis a pre-diagnosis can be established, concluding that the evaluated spectrum is associated with a considerable fault level, since the maximum amplitude of the fault frequency has reached 66.6% of the isolines of the fault evolution map.

4.2 Diagnostic spectra

Bearing vibration signals are not periodic, but stochastic. Therefore, throughout a record there are segments associated with different energy values for the same fault level. This causes changes in the behaviour of the spectrum, especially in the amplitude of the fault frequency and its harmonics.

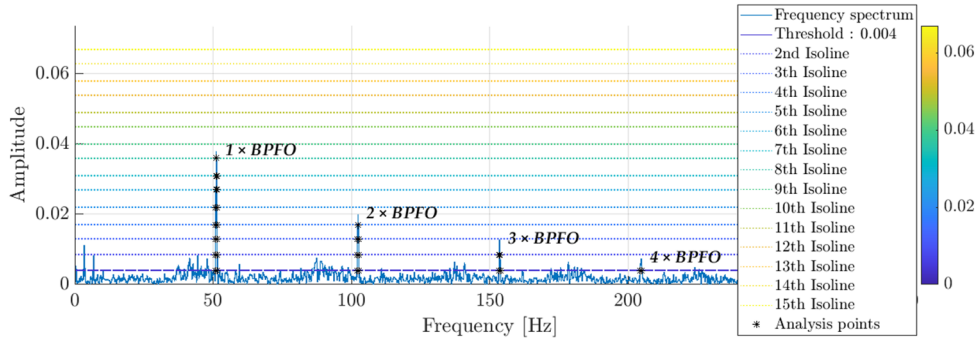

Figure 7: Use of isolines as a fault level scaling pattern (500 rpm recording and fault F2).

Fig. 8 shows two samples of the same record with spectra of different behaviour, at 500 rpm and catalogued with fault level F2. As previously mentioned, the database used corresponds to a combined rolling element (BSF) and outer track (BPFO) fault. Therefore, the spectrum in Fig. 8(a) shows higher energy associated with the BSF component, compared to the spectrum in Fig. 8(b), and vice versa for the BPFO component.

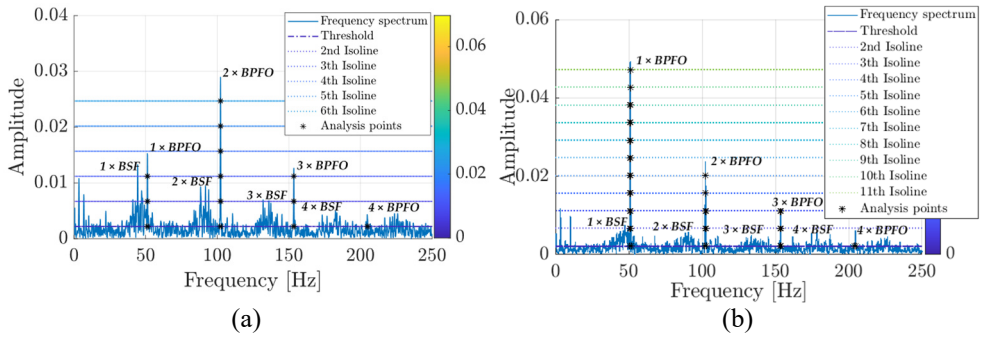

Figure 8: Spectra of two samples (record at 500 rpm and fault F2).

Fig. 9 presents the diagnosis of the spectra presented in Fig. 8. In this figure, despite the differences in the behaviour of the spectrum, the diagnosis has been feasible, which demonstrates the versatility and accuracy of the methodology presented. Fig. 9(a) presents the spectrum diagnostic presented in Fig. 8(a), where the measures of central tendency establish a ratio of 1.95 and 2.08 for the mean and median, which is consistent with the fault level to which more samples correspond. The same is true for the diagnostic spectrum in Fig. 8(a) presented in Fig. 9(a), where a ratio of 2.23 and 2.24 is observed for the mean and median respectively.

4.3 Evaluation of the methodology

In order to estimate the performance of the proposed methodology, the 45 records of the database were diagnosed in their respective fault evolution maps, associated to speeds of 200,

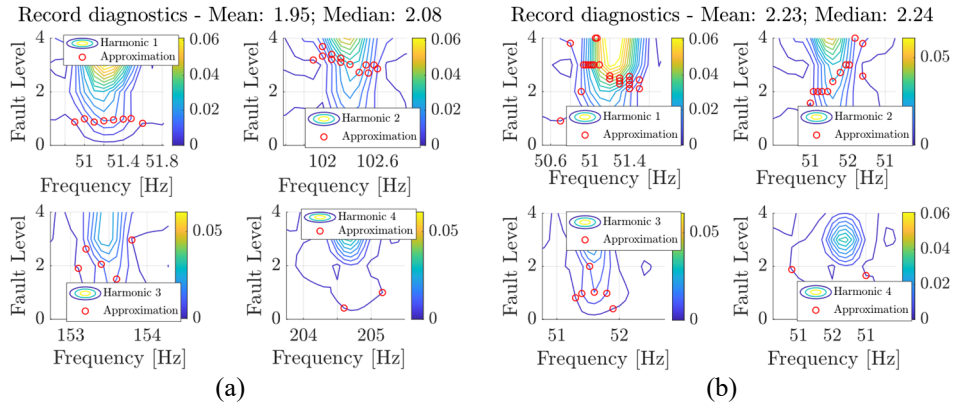

Figure 9: Spectrum diagnostics.

350 and 500 rpm. In each of the records, five samples (of 5 seconds) have been identified that meet the conditions presented in Section 2.3.2. Therefore, the fault evolution maps associated with each rpm will be evaluated using 75 samples, comprising the five fault levels (F0, F1, F2, F3, F4) analysed, including the normal state.

Fig. 10 presents the confusion matrices to evaluate the measures of central tendency used in the estimation of the corresponding failure level. Fig. 10(a) shows that the "mean" has a higher accuracy in the diagnosis of the different samples, reaching 79.11% correct. The samples with failure level F0, F1 and F2 present an error in diagnosis of 13.3, 6.7% and 15.6% respectively. For the misdiagnosed samples, samples with fault level F0 and F1 are associated with a higher fault level, while samples with fault F2 are associated with a lower and higher fault level. In the case of the samples with fault F3, all have been correctly diagnosed. Finally, the samples with fault level F4 are the most problematic, with 68.9% of failures in the diagnosis. A similar behaviour is observed in the median confusion matrix Fig. 10(b), reaching 78.22% correct.

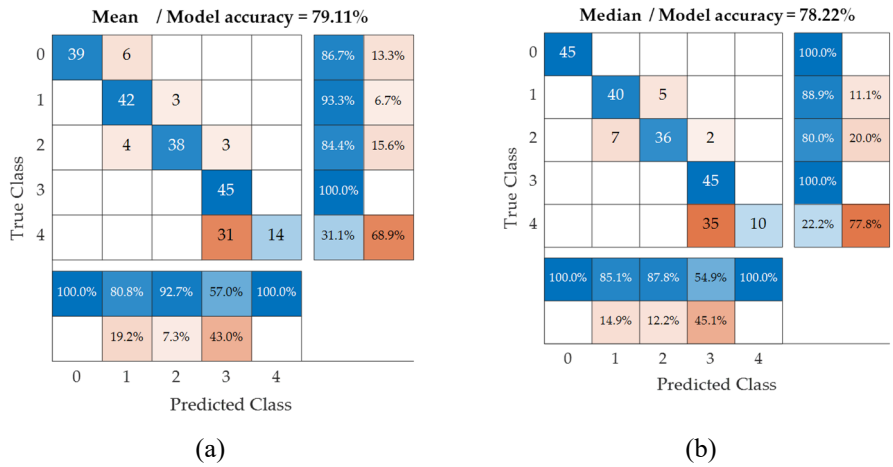

Figure 10: Confusion matrix of measures of central tendency. (a) Mean; and (b) Median.

5 CONCLUSIONS

This paper documents the evaluation of the bearing diagnosis methodology proposed in Soto-Ocampo et al. [14]. It concludes that the implementation of contour maps allows the construction of maps that characterise the evolution of a fault. In addition, it allows future records to be evaluated and associated to a fault level according to the behaviour of the fault frequency and harmonics.

Regarding the process of evaluation and diagnosis of a record, two phases have been distinguished. The first is associated with the consideration of the value of the isolines as a scale map to evaluate the amplitudes of the fault frequency and harmonics of the spectrum under analysis. In this way, a visual analysis of the trend of the amplitudes is carried out, to subsequently carry out the diagnosis and establish the corresponding fault level. In the second phase, the relationship between the analysis points and the coordinates (frequency, amplitude and fault level) of the points of the isolines that make up the fault evolution map can be seen. This, based on the behaviour of the fault frequency amplitudes and harmonics, establishes the corresponding fault level when implementing the measures of central tendency.

The methodology has been validated using 225 samples associated with 45 vibration records obtained from a test bench. In the evaluation of the methodology, an accuracy of around 79% has been observed. It should be noted that this value was obtained by processing all the analysis points of 6 harmonics. Therefore, if an analysis to identify which of the harmonics has the highest relationship with the fault level is considered, the accuracy would be improved. This will be considered in future works.

REFERENCES

[1] Behzad, M., Feizhoseini, S., Arghand, H.A., Davoodabadi, A. & Mba, D., Failure threshold determination of rolling element bearings using vibration fluctuation and failure modes. *Appl. Sci*., **11**, p. 160, 2021. DOI: 10.3390/app11010160.

[2] Shao, H., Jiang, H., Lin, Y. & Li, X., A novel method for intelligent fault diagnosis of rolling bearings using ensemble deep auto-encoders. *Mech. Syst. Signal Process*, **102**, pp. 278–297, 2018. DOI: 10.1016/j.ymssp.2017.09.026.

[3] Zhang, W., Li, C., Peng, G., Chen, Y. & Zhang, Z., A deep convolutional neural network with new training methods for bearing fault diagnosis under noisy environment and different working load. *Mech. Syst. Signal Proces*s, **100**, pp. 439–453, 2018. DOI: 10.1016/j.ymssp.2017.06.022.

[4] Liu, R., Yang, B., Zio, E. & Chen, X., Artificial intelligence for fault diagnosis of rotating machinery: A review. *Mech. Syst. Signal Process*, **108**, pp. 33–47, 2018. DOI: 10.1016/j.ymssp.2018.02.016.

[5] Moshrefzadeh, A., Condition monitoring and intelligent diagnosis of rolling element bearings under constant/variable load and speed conditions. *Mech. Syst. Signal Process*, **149**, 107153, 2021. DOI: 10.1016/j.ymssp.2020.107153.

[6] Randall, R.B. & Antoni, J., Rolling element bearing diagnostics: A tutorial. *Mech. Syst. Signal Process*, **25**, pp. 485–520, 2011. DOI: 10.1016/j.ymssp.2010.07.017.

[7] Brusa, E., Bruzzone, F., Delprete, C., Di Maggio, L.G. & Rosso, C., Health indicators construction for damage level assessment in bearing diagnostics: A proposal of an energetic approach based on envelope analysis. *Appl. Sci*., **10**, p. 8131, 2020. DOI: 10.3390/app10228131.

[8] Hamadache, M., Jung, J.H., Park, J. & Youn, B.D., A comprehensive review of artificial intelligence-based approaches for rolling element bearing PHM: Shallow and deep learning. *JMST Adv*., **1**, pp. 125–151, 2019. DOI: 10.1007/s42791-019-0016-y.

[9] Liu, Z.-H., Lu, B.-L., Wei, H.-L., Chen, L., Li, X.-H. & Ratsch, M., Deep adversarial domain adaptation model for bearing fault diagnosis. *IEEE Trans. Syst. Man Cybern. Syst*., pp. 1–10, 2020. DOI: 10.1109/TSMC.2019.2932000.

[10] Sun, J., Yan, C. & Wen, J., Intelligent bearing fault diagnosis method combining compressed data acquisition and deep learning. *IEEE Trans. Instrum. Meas*., **67**, pp. 185–195, 2018. DOI: 10.1109/TIM.2017.2759418.

[11] Lei, Y., Jia, F., Lin, J., Xing, S. & Ding, S.X., An intelligent fault diagnosis method using unsupervised feature learning towards mechanical big data. *IEEE Trans. Ind. Electron*., **63**, pp. 3137–3147, 2016. DOI: 10.1109/TIE.2016.2519325.

[12] Kwak, D.-H., Lee, D.-H., Ahn, J.-H. & Koh, B.-H., Fault detection of roller-bearings using signal processing and optimization algorithms. *Sensors*, **14**, pp. 283–298, 2013. DOI: 10.3390/s140100283.

[13] Qiu, H., Lee, J., Lin, J. & Yu, G., Robust performance degradation assessment methods for enhanced rolling element bearing prognostics. *Adv. Eng. Inform*., **17**, pp. 127–140, 2003. DOI: 10.1016/j.aei.2004.08.001.

[14] Soto-Ocampo, C.R., Cano-Moreno, J.D., Mera, J.M. & Maroto, J., Bearing severity fault evaluation using contour maps: Case study. *Appl. Sci*., **11**, p. 6452, 2021. DOI: 10.3390/app11146452.

[15] Ghafari, S.H., A fault diagnosis system for rotary machinery supported by rolling element bearings. PhD dissertation, University of Waterloo, 2007.

[16] Yu, K., Lin, T.R., Tan, J. & Ma, H., An adaptive sensitive frequency band selection method for empirical wavelet transform and its application in bearing fault diagnosis. *Measurement*, **134**, pp. 375–384, 2019. DOI: 10.1016/j.measurement.2018.10.086.

[17] Gupta, P. & Pradhan, M.K., Fault detection analysis in rolling element bearing: A review. *Mater. Today Proc*., **4**, pp. 2085–2094, 2017. DOI: 10.1016/j.matpr.2017.02.054.

[18] Guilbert, E., Multi-level representation of terrain features on a contour map. *GeoInformatica*, **17**, pp. 301–324, 2013. DOI: 10.1007/s10707-012-0153-z.

[19] Jeong, M.-G., Lee, E.-B., Lee, M. & Jung, J.-Y., Multi-criteria route planning with risk contour map for smart navigation. *Ocean Eng*., **172**, pp. 72–85, 2019. DOI: 10.1016/j.oceaneng.2018.11.050.

[20] Hahmann, T. & Usery, E.L., What is in a contour map? S.I. Fabrikant, M. Raubal, M. Bertolotto, C. Davies, S. Freundschuh, S. Bell (eds), Springer: Cham, 2015.

[21] Fernández-Francos, D., Martínez-Rego, D., Fontenla-Romero, O. & Alonso-Betanzos, A., Automatic bearing fault diagnosis based on one-class ν-SVM. *Comput. Ind. Eng*., **64**, pp. 357–365, 2013. DOI: 10.1016/j.cie.2012.10.013.

[22] Smith, W.A. & Randall, R.B., Rolling element bearing diagnostics using the Case Western Reserve University data: A benchmark study. *Mech. Syst. Signal Process*, **64–65**, pp. 100–131, 2015. DOI: 10.1016/j.ymssp.2015.04.021.

[23] IS/ISO 13373-2, Condition monitoring and diagnostics of machines: Vibration condition monitoring, Part 2: Processing analysis and presentation of vibration data. Bureau of Indian Standards: New Delhi, India, p. 38, 2005.

[24] Samanta, B. & Al-Balushi, K.R., Artificial neural network based fault diagnostics of rolling element bearings using time-domain features. *Mech. Syst. Signal Process*, **17**, pp. 317–328, 2003. DOI: 10.1006/mssp.2001.1462.

[25] Liu, Z., Jin, Y., Zuo, M.J. & Peng, D., ACCUGRAM: A novel approach based on classification to frequency band selection for rotating machinery fault diagnosis. *ISA Trans*., **95**, pp. 346–357, 2019. DOI: 10.1016/j.isatra.2019.05.007.

[26] Soto-Ocampo, C.R., Mera, J.M., Cano-Moreno, J.D. & Garcia-Bernardo, J.L., Low-cost, high-frequency, data acquisition system for condition monitoring of rotating machinery through vibration analysis-case study. *Sensors*, **20**, p. 3493, 2020. DOI: 10.3390/s20123493.
[27] Rizzo, M.L., *Statistical Computing with R*, CRC Press: Ohio, 2007.
[28] Soto-Ocampo, C.R., Cano-Moreno, J.D., Mera, J.M. & Maroto, J., Bearing database: Combined failure, 2021. DOI: 10.5281/zenodo.5084405.